Virus Research 263 (2019) 34–46

Contents lists available at ScienceDirect

Virus Research

journal homepage: www.elsevier.com/locate/virusres

Integrated analysis of microRNA-mRNA expression in A549 cells infected with influenza A viruses (IAVs) from different host species

Jie Gao[1], Lingxi Gao[1], Rui Li, Zhenping Lai, Zengfeng Zhang, Xiaohui Fan*

Department of Microbiology, School of Preclinical Medicine, Guangxi Medical University, Nanning, 530021, China

ARTICLE INFO

Keywords:
Influenza A
Different host species
MicroRNAs
mRNA
Microarray
High-throughput sequencing

ABSTRACT

Although several miRNAs have been demonstrated to be involved in the influenza virus replication cycle, the identification of miRNAs and mRNAs that are expressed in A549 cells infected with influenza A viruses (IAVs) from different host species has remained poorly studied. To investigate the molecular mechanisms associated with the differential expression of miRNAs during influenza A virus infection, we performed global miRNA and mRNA expression profiling in A549 cells infected with human-origin seasonal influenza A virus H3N2 (Human_Br07), swine-origin influenza A virus H1N1 (SW_3861) or avian-origin influenza A virus H3N2 (AVI_9990). The miRNA and mRNA expression profiles were obtained by microarray and high-throughput sequencing analyses, respectively. The integrated analysis of differentially expressed miRNAs (DEMs) and differentially expressed genes (DEGs) was performed using bioinformatics tools, and the expression of miRNAs and mRNAs was validated by real-time quantitative polymerase chain reaction (RT-qPCR). We identified 20 miRNAs (6 upregulated and 14 downregulated) and 1286 mRNAs (935 upregulated and 351 downregulated) exhibiting the same differential expression trends in three infected groups of cells compared with an uninfected control. An integrated analysis of these expression profiles identified 79 miRNA-mRNA pairs associated with the influenza A reference pathway, and 107 miRNA-mRNA interactions were correlated with the defense of the virus. Additionally, the obtained results were supported by an RT-qPCR analysis of 8 differentially expressed miRNAs (hsa-miR-210-3p, hsa-miR-296-5p, hsa-miR-371a-5p, hsa-miR-762, hsa-miR-937-5p, hsa-miR-1915-3p, hsa-miR-3665, and hsa-miR-1290) and 13 differentially expressed mRNAs (IFNL1, CXCL10, RSAD2, MX1, OAS2, IFIT2, IFI44 L, MX2, XAF1, NDRG1, FGA, EGLN3, and TFRC). Our findings indicate that dysregulated miRNA expression plays a crucial role in infection caused by IAVs originating from different species and provide a foundation for further investigations of the molecular regulatory mechanisms of miRNAs involved in influenza A virus infection.

1. Introduction

Influenza A virus (IAV) is an enveloped negative-sense single-stranded RNA virus belonging to the *Orthomyxoviridae* family. Individuals infected with this virus exhibit several respiratory symptoms, including fever, cough, headache, fatigue, runny nose and sore throat, and in some cases such infections can be fatal (Nicholson et al., 2003), especially in instances of interspecies transmission (Short et al., 2015). Generally, IAV exhibits species specificity, but viruses from other species, including avian and swine viruses, can also infect humans by crossing the species barrier (Kuiken et al., 2006; Van Reeth, 2007). In recent years, IAVs of avian- and swine-origin have caused death in several cases and present a severe threat to human health (Sun et al., 2018; Zhou et al., 2018). Besides, IAVs of human-origin cannot be ignored, as the seasonal virus may cause 290,000–650,000 deaths each year (http://www.who.int/news-room/detail/14-12-2017-up-to-650-000-people-die-of-respiratory-diseases-linked-to-seasonal-flu-each-year, Accessed 9 January 2019) and has resulted in serious physical and economic burdens on the human population. Although the pathogenic mechanisms of IAVs have continued to be studied, few investigations have simultaneously studied the pathogenicity of IAVs from different species. In this study, three IAVs from different species were used to infect human lung carcinoma cells (A549) to study common aspects of their pathogenicity.

MicroRNAs (miRNAs) are endogenous, small (17–24 nucleotides in length) noncoding RNAs that have been identified in animals, plants

* Corresponding author: Xiaohui Fan, Department of Microbiology, School of Preclinical Medicine, Guangxi Medical University, 22 Shuangyong Road, Nanning, 530021, China.
E-mail address: fanxiaohui63@163.com (X. Fan).
[1] The first two authors contributed equally to the work.

https://doi.org/10.1016/j.virusres.2018.12.016
Received 17 September 2018; Received in revised form 22 December 2018; Accepted 28 December 2018
Available online 31 December 2018
0168-1702/

and some viruses (Bartel, 2004; Carthew and Sontheimer, 2009; Grundhoff and Sullivan, 2011), regulating target gene expression at the posttranscriptional level via mRNA degradation or translational repression (Turchinovich et al., 2012). As of March of 2018, 48,885 human mature miRNAs were registered in the miRBase 22 release, and the number of newly discovered miRNAs is still growing. For influenza virus, only one study has reported on an IAV-encoded microRNA-like small RNA (miR-HA-3p), which is encoded by an H5N1 virus (Li et al., 2018), with most miRNAs involved in influenza virus infection being produced by host cells. Previous studies showed that miRNAs have key regulatory roles in cellular biological processes, including cell proliferation, differentiation, metabolism and apoptosis (Bartel, 2004; Zhang et al., 2018b) as well as in regulating disease development, such as cancer formation, and pathogen infection (Hill and Tran, 2018; Holla and Balaji, 2015; Trobaugh and Klimstra, 2017). Recently, many studies have reported that the expression profiles of host miRNAs are altered upon infection by IAVs, demonstrating that some miRNAs may participate in the influenza virus infection process. For example, let-7c, miR-323, miR-491, miR-654, miR-3145, miR-584-5p and miR-1249 have been reported to target the viral genes M1, PB1 or PB2 to directly inhibit viral replication (Khongnomnan et al., 2015; Ma et al., 2012; Song et al., 2010; Wang et al., 2017). In addition, miR-21-3p, miR-144, miR-146a, miR-203, miR-302 and miR-483-3p were shown to target host genes to indirectly mediate the antiviral response by inducing the generation of immune factors (Chen et al., 2017; Deng et al., 2017; Maemura et al., 2018; Rosenberger et al., 2017; Xia et al., 2018; Zhang et al., 2018a). In 2012, Emma-Kate Loveday et al. provided the first experimental evidence demonstrating the complex temporal and strain-specific regulation of the host microRNAome by pandemic S-OIV and deadly A-OIV-host infections in human cells (Loveday et al., 2012). Subsequently, Jarika Makkoch et al. investigated the miRNA expression profiles of A549 cells infected with different influenza virus subtypes (pH1N1, H3N2 and H5N1) (Makkoch et al., 2016). However, to date, a comprehensive analysis of miRNAs and mRNAs that are commonly expressed in A549 cells infected with different typical influenza viruses from a variety of species sources has not been reported.

In this study, we performed global miRNA and mRNA expression profiling in A549 cells infected with three types of IAVs from different host species (human, swine and avian origin) and explore the molecular regulatory pathways of miRNAs with common expression patterns among the three IAVs infection, which may be involved in the IAV infection process. In addition, real-time quantitative polymerase chain reaction (RT-qPCR) was used to test whether the expression of miRNAs and mRNAs was consistent with the results of the microarray and high-throughput sequencing analyses. The findings of this study provide novel insights into anti-IAV mechanisms and may be helpful in guiding research aimed at delineating broad-spectrum antiviral targets for pandemic influenza control.

2. Materials and methods

2.1. Cell culture and virus infection

The human lung carcinoma cells (A549) used in this study were cultured in Kaighn's modification of Ham's F-12 K Medium (F12 K; Gibco) supplemented with 10% FBS and 1% penicillin-streptomycin in a 37°C incubator with 5% CO_2. The influenza viruses A/Brisbane/10/2007(H3N2), A/Duck/Shantou/9990/2010(H3N2) and A/Swine/Guangxi/3861/2011(H1N1) were propagated in specific pathogen-free (SPF) embryonated eggs. The harvested viruses were stored at −80°C prior to use. All viruses were titrated on Madin-Darby canine kidney (MDCK) cells to determine pfu/mL, and the viruses were diluted with F12 K medium to a multiplicity of infection (MOI) of 1.

A549 cells were seeded in a 6-well plate at a density of 5×10^3 cells per well. When the cell density reached approximately 80%, the cell culture medium was removed and cells were washed with 2 mL of phosphate buffered saline (PBS). Next, suspensions of the three different viruses were added separately into each well (500 μL/well) and cultured in 5% CO_2 at 37°C for 2 h. Subsequently, the viral suspensions were removed from each well and the cells were washed with PBS. Finally, F12 K medium supplemented with TPCK-treated trypsin (1 μg/ml) was added to each well and incubated for 24 h.

2.2. Agilent miRNA microarray and miRNA data analyses

After a 24 h infection, the culture medium was removed from each well and cells were lysed with 600 μL of lysis/binding buffer. The total RNA from the cells was extracted with a mirVanaTM RNA Isolation Kit (Ambion) following the manufacturer's protocol. The RNA was spectrophotometrically analyzed using a NanoDrop ND-2000 (Thermo Scientific) and an Agilent Bioanalyzer 2100 (Agilent Technologies) to assess RNA quality. Next, the total RNA samples from the four groups (uninfected cells, Human_Br07 infected cells, AIV_9990 infected cells, and SW_3861 infected cells) were diluted with Tris-EDTA buffer (1×, pH 7.5) to a final concentration of 50 ng/μL. Subsequently, the following steps were performed for the miRNA microarray assay. First, the total RNA sample was dephosphorylated and denatured following to the manufacturer's instructions. The miRNAs were labeled with cyanine 3-cytidine bisphosphate (pCp) by ligation, and the labeled miRNAs were then purified using a Micro Bio-Spin 6 column (Bio-Rad). Next, the miRNAs were hybridized to the microarray at 55°C for 20 h, and the microarray was subsequently washed twice and scanned with an Agilent scanner.

Feature Extraction (version 10.7.1.1, Agilent Technologies) was used to analyze array images to obtain the raw data. GeneSpring (version 14.8, Agilent Technologies) was used to perform basic analyses with the raw data, and the raw data was normalized using the quantile algorithm. The probes that were present in at least 100.0% of the samples from any 1 condition (out of 2 conditions) were flagged as "Detected" and were used for further analyses. Next, differentially expressed miRNAs were identified by determining the fold changes, with *p*-values calculated using t-tests. The threshold values for differentially expressed miRNAs were a p-value of < 0.05 and a fold change of > 2 or < 0.5. Next, the target genes of the differentially expressed miRNAs were predicted using three databases (TargetScan, microRNAorg, PITA). Finally, hierarchical clustering was performed to assess the distinguishable miRNA expression pattern among 12 samples.

2.3. Library construction, mRNA sequencing and analysis

After extraction of total cell RNA, DNA were removed by DNase digestion, the mRNAs were enriched with oligo(dT) magnetic beads, and short mRNA fragments were generated by adding fragmentation buffer. Next, we used these short mRNA fragments as template to synthesize first-strand cDNA using random primers, followed by the synthesis of second-strand cDNA. Subsequently, the double-stranded DNA was purified using a Qubit dsDNA assay kit, and the purified DNA was 3′-adenylated, ligated with sequencing adapters, and used for PCR amplification. An Agilent 2100 Bioanalyzer (Agilent Technologies, Santa Clara, CA, USA) was used to evaluate RNA integrity, and samples with an RNA Integrity Number (RIN) of ≥ 7 were used in subsequent analyses. Finally, the libraries were sequenced on an Illumina sequencing platform (HiSeqTM 2500 or Illumina HiSeq X Ten) and 125 bp/150 bp paired-end reads were generated.

To analyze the mRNA sequencing data, the NGS QC Toolkit (Patel and Jain, 2012) was used to process the raw data, and the reads containing poly-N and low quality reads were removed to obtain the clean reads. The clean reads were mapped to the reference genome using hisat2 (Kim et al., 2015). Next, the FPKM (Trapnell et al., 2010) value of each gene was calculated using cufflinks (Roberts et al., 2011), and the read count for each gene was obtained using htseq-count (Anders et al., 2015). DEGs were identified using the DESeq (Anders and Huber,

2012) R package functions estimateSizeFactors and nbinomTest. A *p*-value of < 0.05 and a fold change > 2 or < 0.5 was set as the threshold for significantly differential expression. Finally, GO enrichment and KEGG (Kanehisa et al., 2008) pathway enrichment analyses of the DEGs were performed using R based on the hypergeometric distribution, and the expression patterns of DEGs common to the different samples were also shown by hierarchical clustering.

2.4. Integrated analysis of miRNA and mRNA expression profiles

The common DEMs and DEGs were screened using the *VennDiagram* package based on the DEMs and DEGs identified from three infected groups compared with the uninfected group. Next, the miRNA-mRNA interactions related to IAV infection were determined using R based on the target gene prediction results of miRNAs and the biological function analyses of DEGs. Finally, the networks of miRNA and mRNA expression profiles were displayed using Cytoscape version 3.0.1.

2.5. Real-time quantitative PCR of mRNA and miRNA

To validate the results of the microarray and high-throughput sequencing analyses, we chose 8 differentially expressed miRNAs and 13 mRNAs for RT-qPCR analysis. Total RNA was extracted from three infected groups and one uninfected group using a mirVanaTM RNA Isolation Kit (Ambion) following the manufacturer's specifications. For the mature miRNAs, cDNA synthesis was performed using a QuantiTect Reverse Transcription Kit (Qiagen), and for the mRNA, HiScript II Q RT SuperMix for qPCR (Vazyme) was used to synthesize the cDNA. Real-time PCR for miRNA and mRNA was performed using a LightCycler® 480 II Real-time PCR instrument (Roche, Swiss). Reactions were incubated in 384-well optical plates (Roche, Swiss) at 95 °C for 5 min, followed by 40 cycles of 95 °C for 10 s and 60 °C for 30 s, with each sample was run in triplicate. At the end of the PCR cycles, melting curve analysis was performed to validate the specific generation of the expected PCR product. The microRNA-specific primer sequences were designed in the laboratory and synthesized by Generay Biotech (Generay, PRC) based on the miRNA sequences obtained from the miRBase database (Release 20.0), while the mRNA primer sequences were designed based on the mRNA sequences obtained from the NCBI database (Supplementary material). The microRNAs and mRNA expression levels were normalized to the reference genes (RNU6B and Human ACTB, respectively) and calculated using the 2-ΔΔCt method (Livak and Schmittgen, 2001).

3. Results

3.1. miRNA expression profiling

To identify changes in miRNA expression in A549 cells infected with influenza A virus, four groups were assayed, including the Human_Br07 H3N2-infected group, the AVI_9990 H3N2-infected group, the SW_3861 H1N1-infected group and an uninfected group. Each group was assayed in triplicate, and 12 small RNA libraries were constructed for miRNA expression profiling. Agilent Human miRNA Microarrays (Release 21.0) provided 2549 human miRNA probes. The DEMs of the three infected groups were screened and displayed using volcano plots (Fig. 1A), which showed that compared with the uninfected group, 64, 42 and 35 DEMs were detected in A549 cells infected with the Human_Br07 H3N2 virus (26 upregulated and 38 downregulated), the AVI_9990 H3N2 virus (20 upregulated and 22 downregulated), and the SW_3861 H1N1 virus (11 downregulated and 24 upregulated), respectively. A greater number of upregulated than downregulated miRNAs were detected in the three groups, indicating that the miRNAs in A549 cells were primarily downregulated after IAV infection. Furthermore, viruses isolated from different species exhibited specific DEMs, with 25, 8 and 7 specific DEMs detected for cells infected with the Human_Br07, AVI_9990, and SW_3861viruses, respectively (Fig. 1B). Meanwhile, the DEMs that were common to the three infected groups compared with uninfected group were also obtained through a *VennDiagram* analysis using on the above data. Twenty identified DEMs were common to the three groups of A549 cells infected with the three IAVs of different origin, including 14 downregulated and 6 upregulated miRNAs, which were displayed in a Venn diagram (Fig. 1B). In addition, hierarchical clustering analysis (HCA) was used for expression profiling of the DEMs common to the different samples (Fig. 1C). The HCA produced clusters of the 20 miRNAs common to the 12 assayed samples, which were divided into two major branches comprising one uninfected group and 3 infected groups. This result suggested that the expression patterns of these DEMs that were common to the three infected groups were similar and consistent but were distinct from each other.

3.2. mRNA expression profiling

We constructed 12 libraries with different indices for high-throughput sequencing of mRNAs from the different groups, with these data analyzed by RNA-Seq analysis in parallel. The DEGs identified from the three viral infection groups compared with the uninfected group are shown in volcano plots (Fig. 2A). The results showed that compared with the uninfected group, A549 cells infected with the Human_Br07 H3N2, AVI_9990 H3N2 or SW_3861 H1N1 viruses exhibited 3539 DEGs (2262 upregulated and 1277 downregulated), 2272 DEGs (1405 upregulated and 867 downregulated), and 1874 DEGs (1326 downregulated and 548 upregulated), respectively. In contrast to the miRNA expression profiling results, a greater number of upregulated than downregulated mRNAs were detected in the three groups. After analyzing the DEGs using *VennDiagram*, we identified 1286 DEGs that were common to the three infected groups (935 upregulated, 351 downregulated), while each group also has its own specific DEGs, as clearly observed by a Venn diagram (Fig. 2B). In addition, hierarchical clustering analysis was performed to assess the expression profiles of these common differentially expressed mRNAs in different groups, the results of which are shown in a heatmap (Fig. 2C). The diagrams indicate that the mRNA expression profiles of the viral infected groups have significant differences compared with the uninfected group but that the mRNA expression trends observed in the three groups were concordant.

3.3. Bioinformatic analysis of DEMs and DEGs

Three databases (TargetScan, microRNAorg, and PITA) were used to predict the target genes of the identified DEMs. Subsequently, with the goal of elucidating the regulatory pathways and functions of the miRNAs differentially expressed in humans in response to IAV infections, the intersectional DEGs of the three groups compared with the negative control were subjected to further gene function analysis. The DAVID gene annotation tool was used to predict the functions of the DEGs and resulted in the identification of 5598 GO terms, including 3966 in biological process, 521 in cellular component and 1111 in molecular function. The top 10 GO enrichment terms in each category are shown in a bar diagram (Fig. 3), 10 of which were directly associated with the IAV infection, including interferon-beta production, T cell activation, type I interferon signaling pathway, defense response to virus, interferon-gamma-mediated signaling pathway, negative regulation of viral genome replication, inflammatory response, 2′-5′oligoadenylate synthetase activity, chemokine activity and cytokine activity. In addition, a KEGG pathway enrichment analysis was performed that identified 271 KEGG pathway terms, with the top 20 items displayed in a bubble diagram (Fig. 4). Ten of these items are directly associated with the infection of IAVs, including the influenza A pathway, TNF signaling pathway, Jak-STAT signaling pathway, cytosolic DNA-sensing pathway, RIG-I-like receptor signaling pathway, Toll-like receptor signaling pathway, complement and coagulation cascades, NF-kappa B

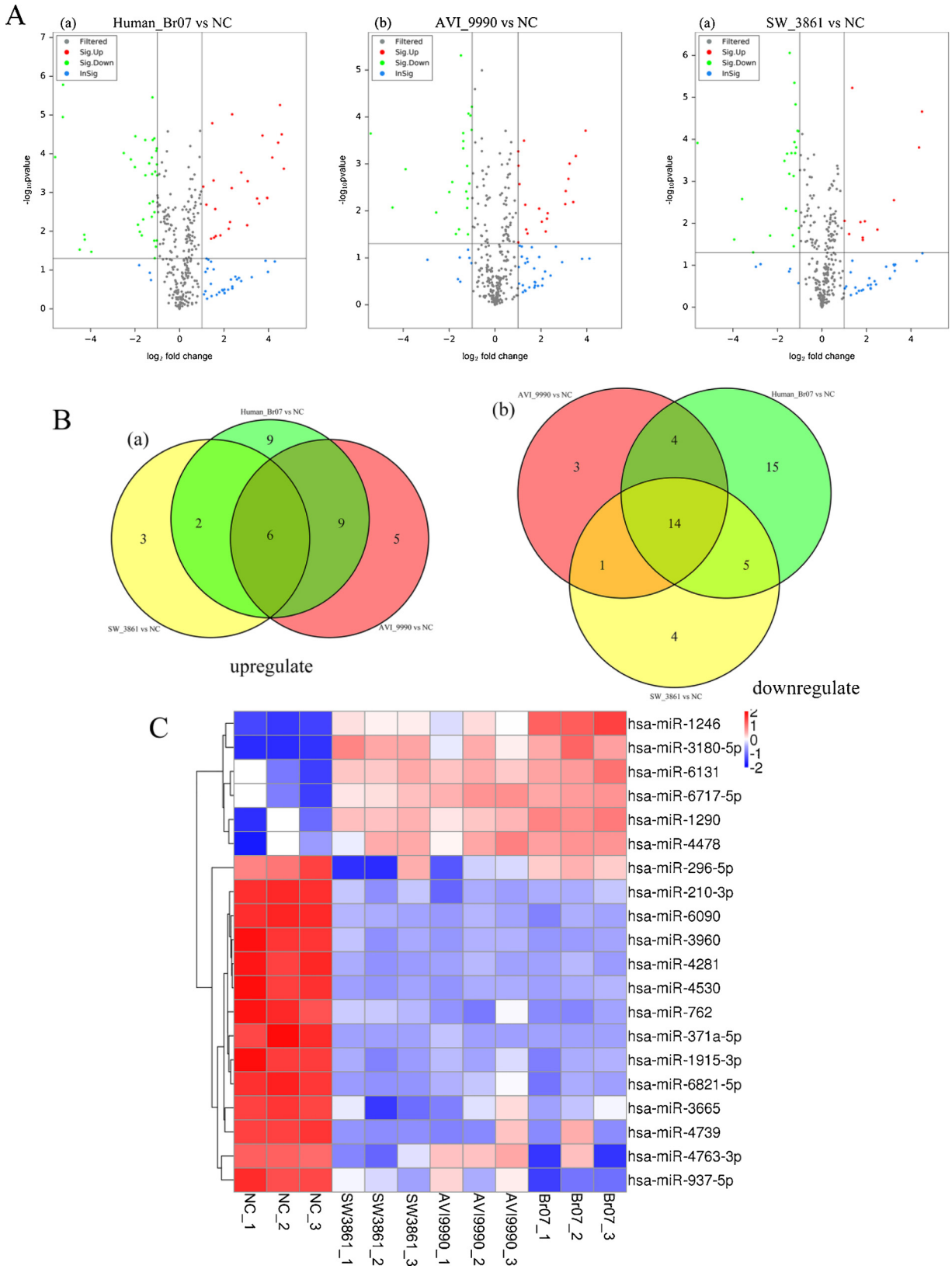

Fig. 1. The expression profiling of miRNAs in the IAV-infected and control groups. **A**. The volcano plot displaying the distribution of DEMs in different infected groups compared with the uninfected group. Green and red dots indicate significantly downregulated and upregulated miRNAs, respectively. **A(a).** 64 DEMs in A549 cells infected with human-origin H3N2 (Human_Br07). **A(b)**. 42 DEMs in A549 cells infected with avian-origin H3N2 (AVI_9990). **A(c)**. 35 DEMs in A549 cells infected with swine-origin H1N1 (SW_3861).**B.** Venn diagram shows the 20 DEMs that are common to the three infected groups: AVI_9990 vs NC (Red Circle), Human_Br07 vs NC (Green Circle), SW_3861 vs NC (Yellow Circle). **B(a)**. Six miRNAs were commonly upregulated in three infected groups. **B(b)**. Fourteen miRNAs were commonly downregulated in three infected groups. **C.** Heat map showing the hierarchical clustering of common miRNAs of 12 samples. Red and blue indicate higher and lower expression in A549 cells, respectively. Abbreviations: IAV, influenza A virus; DEMs, differentially expressed miRNAs; NC, normal control; AVI, avian; SW, swine.

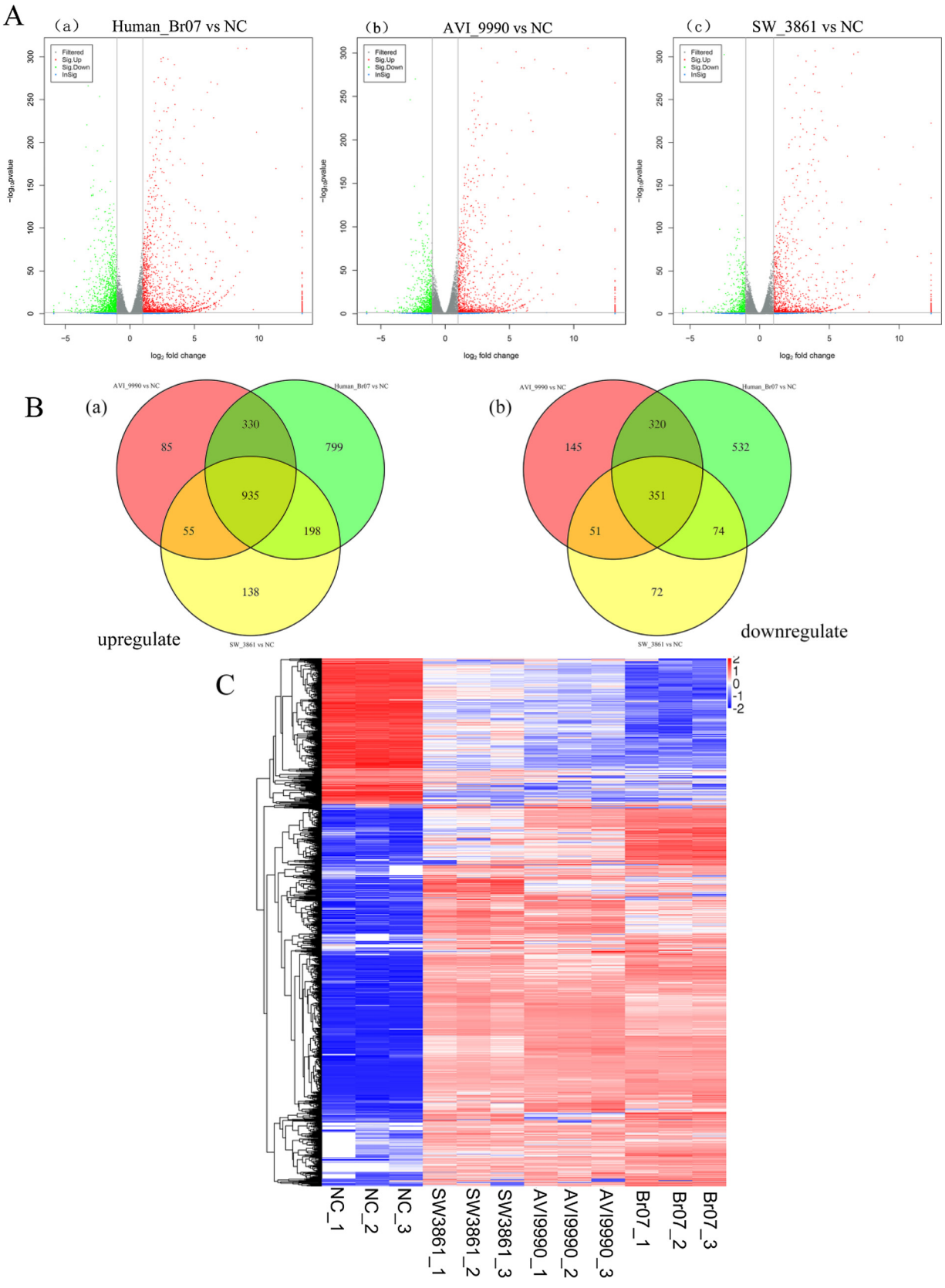

(caption on next page)

signaling pathway, chemokine signaling pathway and cytokine-cytokine receptor interaction. The KEGG map shows that 33 common DEGs participate in the influenza A reference pathway (Fig. 5), and the expression of these mRNAs was upregulated in the three groups.

Fig. 2. The expression profiling of mRNAs in the IAV-infected and control groups. **A.** The volcano plot displaying the distribution of DEGs in different infected groups compared with the uninfected group. Green and red dots indicate significantly downregulated and upregulated genes, respectively. **A(a).** The 3539 identified DEGs in A549 cells infected with human-origin H3N2 (Human_Br07). **A(b).** The 2272 identified DEGs in A549 cells infected with the avian-origin H3N2 (AVI_9990). **A(c).** The 1874 identified DEGs in A549 cells infected with swine-origin H1N1 (SW_3861). **B.** Venn diagram showing the 1286 DEGs that are common to the three infected groups: AVI_9990 vs NC (Red Circle), Human_Br07 vs NC (Green Circle), and SW_3861 vs NC (Yellow Circle). **B(a).** Nine hundred thirty-five mRNAs were commonly upregulated in three infected groups. **B(b).** Three hundred fifty-one mRNAs were commonly downregulated in three infected groups. **C.** Heat map showing the hierarchical clustering of mRNAs that are common to the 12 samples. Red and blue indicate higher and lower expression in A549 cells, respectively. Abbreviations: IAV, influenza A virus; DEGs, differentially expressed genes; NC, normal control; AVI, avian; SW, swine.

3.4. Integrated analysis of miRNA and mRNA expression profiles

We performed an integrated analysis with the above data, including the target genes of DEMs and the expression profiles of the identified DEMs and DEGs. The miRNA-mRNA pairs were acquired from the 20 DEMs and 479 overlapping genes common to the three infected groups. In the three infected groups 1852 common miRNA-mRNA interactions were identified. These miRNA-mRNA pairs may be closely associated with numerous signal pathways and biological processes during the IAV infection. In our study, because numerous miRNAs were observed to be involved in IAV infection, only two items directly related to IAVs were selected to display. These two items, the influenza A pathway and the defense of the virus, were visualized using Cytoscape (Fig. 6), which showed that 79 miRNA-mRNA pairs participated in the influenza A reference pathway and 107 miRNA-mRNA pairs were related to the defense of virus. In Fig. 6, the expression trends of each miRNA and its target mRNA gene are opposite. Furthermore, these miRNA-mRNA interaction diagrams show complex regulatory relationships between the miRNAs and mRNAs that are not simple one-to-one regulatory relationships.

3.5. Validation by RT-qPCR

We selected 8 miRNAs (hsa-miR-210-3p, hsa-miR-296-5p, hsa-miR-371a-5p, hsa-miR-762, hsa-miR-937-5p, hsa-miR-1915-3p, hsa-miR-3665, hsa-miR-1290) and 13 mRNAs (IFNL1, CXCL10, RSAD2, MX1, OAS2, IFIT2, IFI44 L, MX2, XAF1, NDRG1, FGA, EGLN3, TFRC) for further verification. The RT-qPCR results were consistent with the microarray and high-throughput sequencing results (Fig. 7). Among them, the expression levels of CXCL10 and IFNL1 were approximately 20,000-fold higher than in the uninfected control, indicating that they are key genes for the human response to IAVs. In addition, although the results showed that four miRNAs (hsa-miR-210-3p, hsa-miR-762, and hsa-miR-3665) were downregulated and one miRNA (hsa-miR-1290) was upregulated in the three infected groups, the relative expression of these miRNAs was different in the three groups ($p < 0.01$, one-way ANOVA), while the expression of other miRNAs was not significantly different. At the same time, four mRNAs (IFNL1, CXCL10, OAS2, and XAF1) were upregulated and FGA was downregulated in the three infected groups ($p < 0.05$, one-way ANOVA), but the relative expression of these mRNAs was different in the three groups. These results suggest that although the expression trends of some miRNAs and mRNAs were the same in the three infected groups, the relative expression levels were different due to different sources of the viruses. Moreover, after an integrated analysis, we observed that these 8 miRNAs and 13 mRNAs also had a complex regulatory relationship during IAV infection (Table 1), with the results shown in Table 1 corresponding to those shown in Fig. 7.

4. Discussion

IAV infection is a constant threat to humans, and many studies have indicated that miRNAs play key roles in the IAV infection process (Buggele et al., 2012; Peng et al., 2018). However, there is a lack of

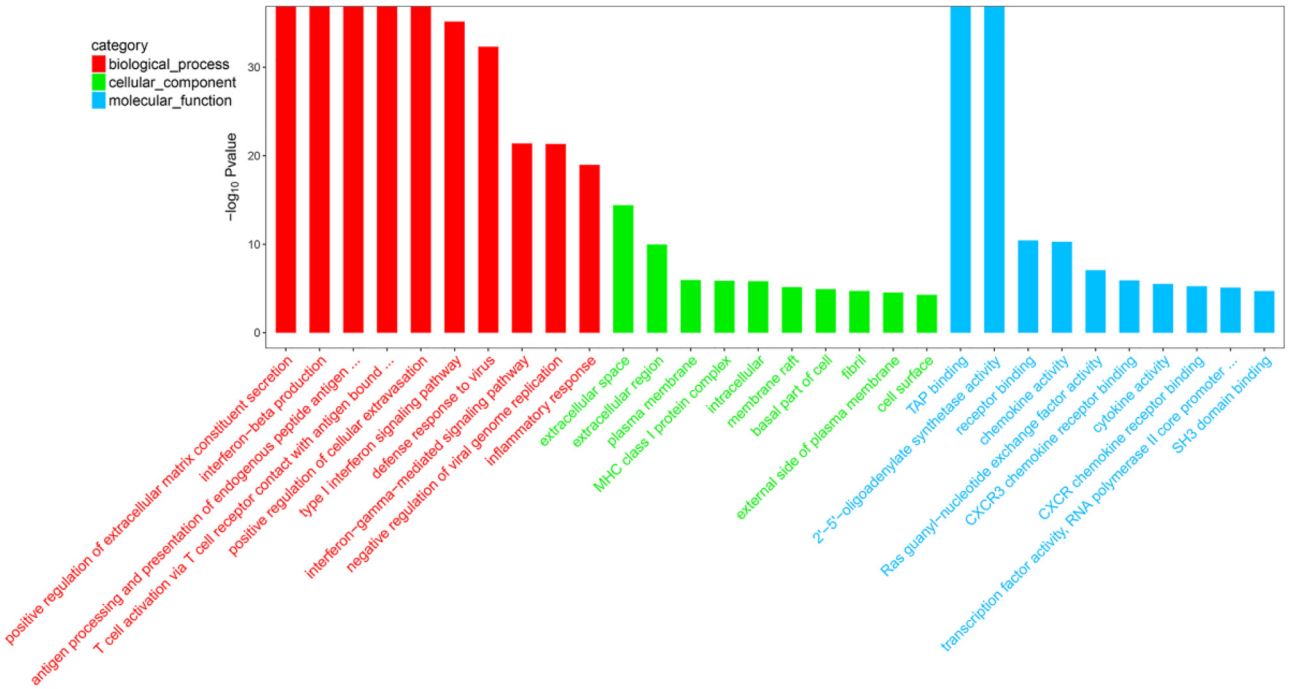

Fig. 3. GO analysis for DEGs identified in the three infected groups. The bar diagram displaying the top 10 GO terms of each category (ListHits > 2 and sort by -log10$^{P-value}$ from high to low), the x-axis shows significantly enriched GO terms, and the y-axis shows the -log10$^{P\text{-}value}$ of these terms. The red, green and blue bars represent 'Biological Process' (BP), 'Cellular Component' (CC), and 'Molecular Function' (MF) categories in GO, respectively. Abbreviations: GO, gene ontology; DEGs, differentially expressed genes.

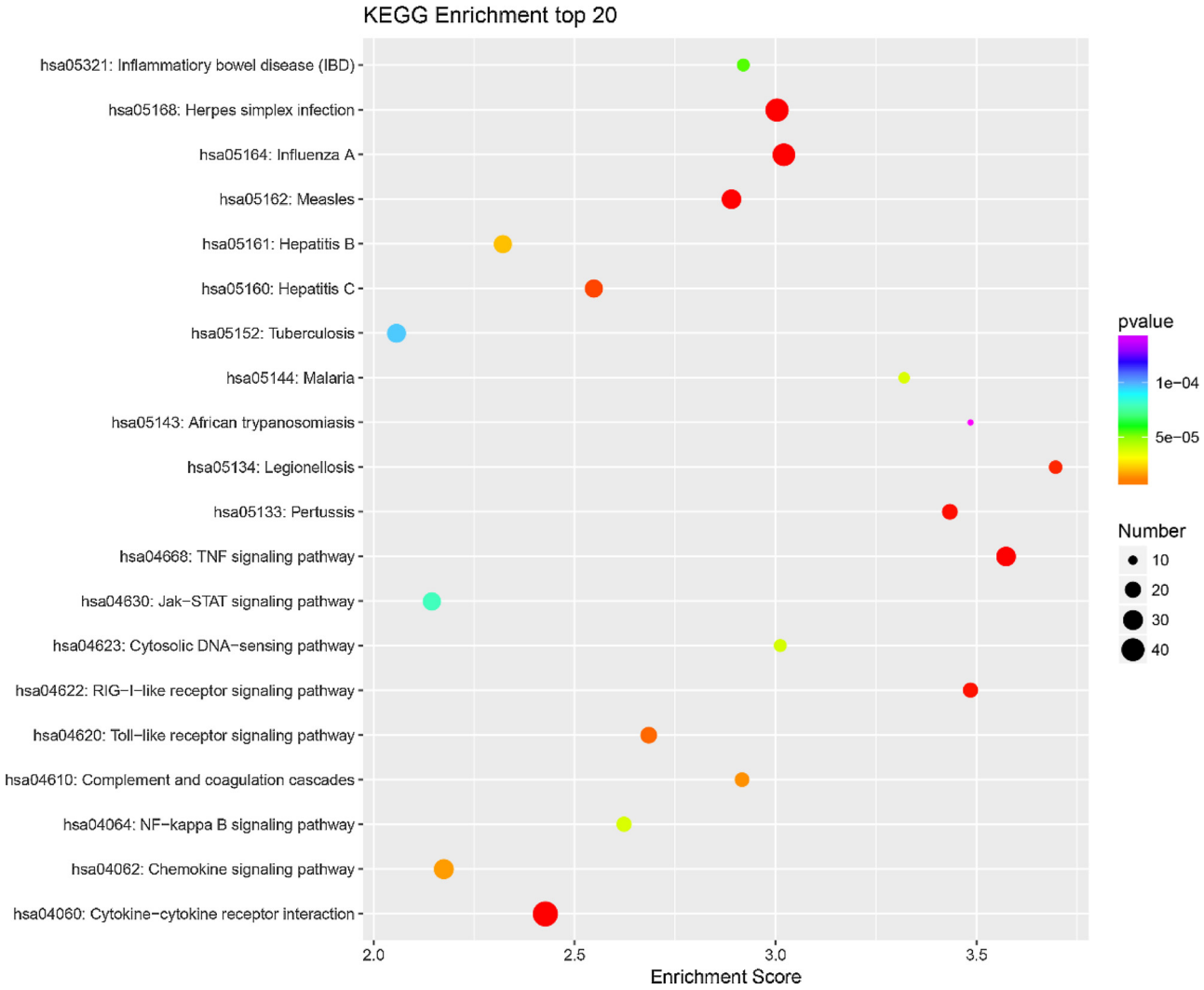

Fig. 4. KEGG pathway analysis for the DEGs identified to be common to the three infected groups. The bubble diagram displays the top 20 items (ListHits > 2 and sort by -log10$^{P-value}$ from high to low), the x-axis shows the score of enrichment, and the y-axis shows significantly enriched pathway terms. The size of each circle represents the number of genes enriched for the given pathway, where the larger the bubble, the more differentially expressed genes are contained, and the color corresponds to the *p*-value, with the bubble color changing from purple-blue-green-red indicating that the enriched *p*-value gradually decreases and the degree of significance gradually increases. Abbreviations: KEGG, Kyoto Encyclopedia of Genes and Genomes; DEGs, differentially expressed genes.

research on miRNAs involved in infections by IAVs originating from different species, and few integrated analyses of DEMs and DEGs during IAV infections have been performed. In our study, we identified 20 miRNAs and 1286 mRNAs that are differentially expressed in A549 cells infected by all three assayed IAVs from different host species. The GO and KEGG analyses showed that 107 miRNA-mRNA interactions were correlated with the defense of the virus, and 79 miRNA-mRNA interactions were involved in the influenza A reference pathway. In addition, we verified that the expression of 8 miRNAs and 13 mRNAs was in accord with the microarray and high-throughput sequencing results. These miRNAs may be highly correlated with IAV infection in A549 cells, potentially providing new insights toward the development of broad-spectrum antiviral targets based on miRNA research.

Numerous studies have shown that human miRNA expression profiles are altered after invasion by influenza virus, and several miRNAs have been shown to participate in the IAV infection process. According to the results of the present study, most miRNAs target human mRNAs associated with the immune system (Chen et al., 2017; Lin et al., 2017; Maemura et al., 2018), with these miRNAs regulating the expression of target mRNAs at the posttranscriptional level to defend against the invading virus. The results of a previous study showed that hsa-miR-937-5p was downregulated in H7N9 patient serum samples compared to its expression in healthy controls using a miRNA microarray analysis (Peng et al., 2017). Another study revealed that hsa-miR-1290 was upregulated in A549 cells that were infected by H1N1 (A/WSN/33) virus and invented a method based on an oligonucleotide complementary to a corresponding segment of the nucleotide sequence of microRNA-1290. This method could be used to diagnose and treat influenza (Shih, 2017). In our study, the gene expression profiling and RT-qPCR verification results showed that hsa-miR-937-5p was downregulated and hsa-miR-1290 was upregulated dramatically in the three infected groups, supporting the results of previous studies. However, other miRNAs have been considered to be regulators that can bind the target influenza virus genes to degrade or inhibit their mRNA expression, blocking influenza virus replication or reducing virulence by inhibiting the expression of viral proteins (Khongnomnan et al., 2015; Ma et al., 2012; Zhang et al., 2017). Although the miRNAs identified in this study that were commonly expressed among the three infected groups had not previously been reported to target the viral genome, whether these miRNAs can directly target viral genes should be further studied.

In this study, we obtained the miRNA expression profiles of A549 cells infected with three influenza viruses through a miRNA microarray

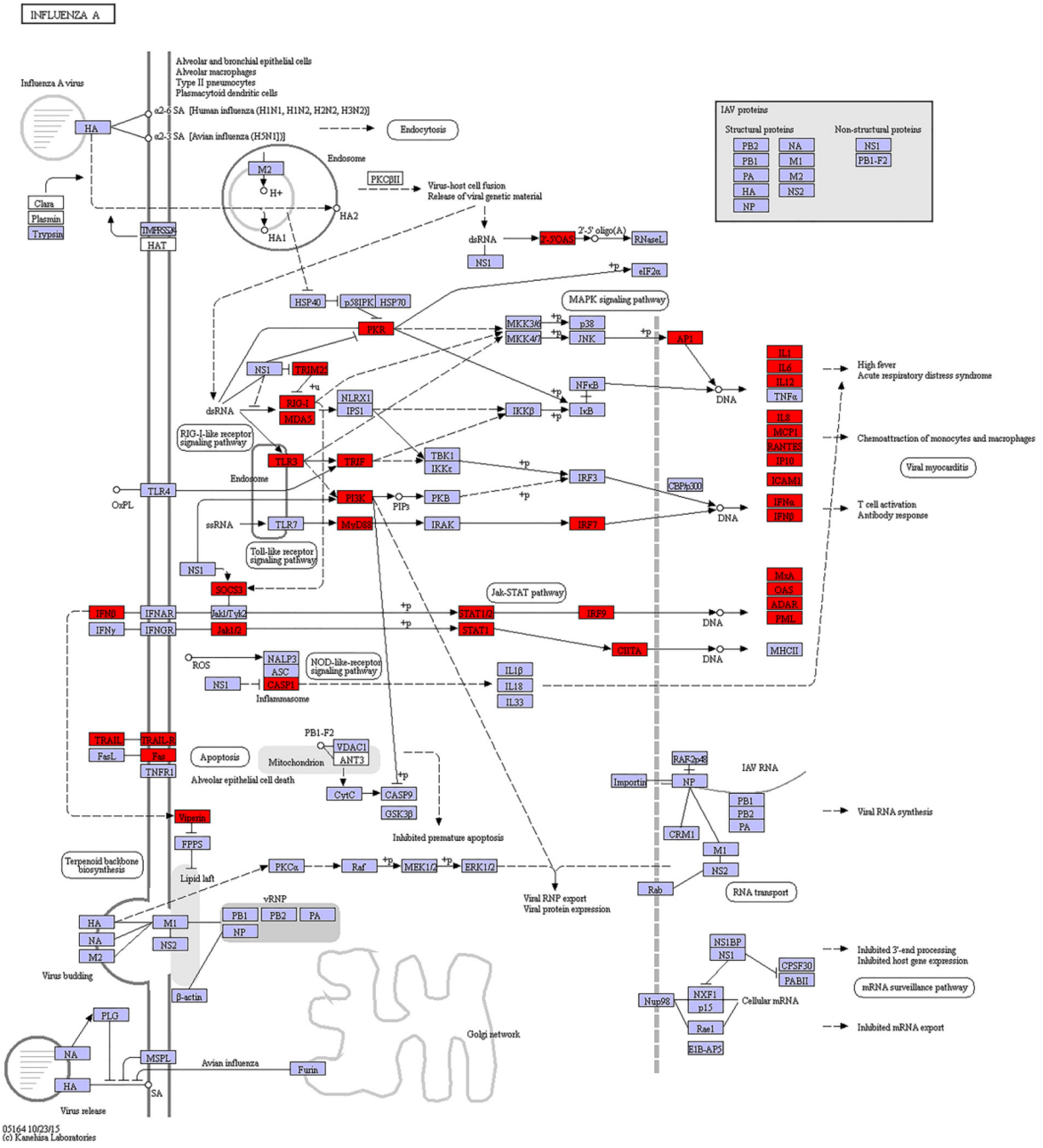

Fig. 5. DAVID KEGG pathway analysis, showing the DEGs (red) that are common to the three infected groups and are involved in the influenza A pathway. Abbreviation: DAVID, The Database for Annotation, Visualization and Integrated Discovery; KEGG, Kyoto Encyclopedia of Genes and Genomes; DEGs, differentially expressed genes.

analysis. Compared to the miRNA profiling results of previous studies, a number of differentially expressed miRNAs were identified that were specific or common to the three infected groups. In the study by Emma-Kate Loveday et al., A549 cells were infected with swine-origin infA (S-OIV) pandemic H1N1 (2009) and avian-origin infA (A-OIV) H7N7 (2003) viruses, and a Geniom miRNA *Homo sapiens* biochip was used to reveal temporal and strain-specific miRNA fingerprints in these two groups of infected cells (Loveday et al., 2012). In addition, four differentially expressed miRNAs in their A-OIV infection group, including hsa-miR-224, hsa-miR-21, hsa-miR-29b and hsa-miR-193b, were also identical in our avian-origin H3N2 (AVI_9990) infection group. The above results suggest that the differential expression of these miRNAs may be associated with IAV infection, since these differentially expressed miRNAs are expressed in cells infected with different virus types and may play an important regulatory role in the IAV infection process. Furthermore, in another study by Jarika Makkoch et al., the differentially expressed miRNAs in A549 cells infected with different subtypes of influenza virus (pH1N1, H3N2 and H5N1) were identified by high-throughput sequencing (Makkoch et al., 2016). Through a comparison analysis, we observed that hsa-miR-26b and hsa-miR-455 are both differentially downregulated in their human-origin seasonal H3N2 infection group and our human-origin H3N2 (Human_Br07) infection group. In addition, hsa-miR-222 expression was upregulated to different degrees in their avian-origin H5N1 infection group and our avian-origin H3N2 (AVI_9990) infection group. Our results agree with theirs, showing that viral subtypes have little effect on the differential

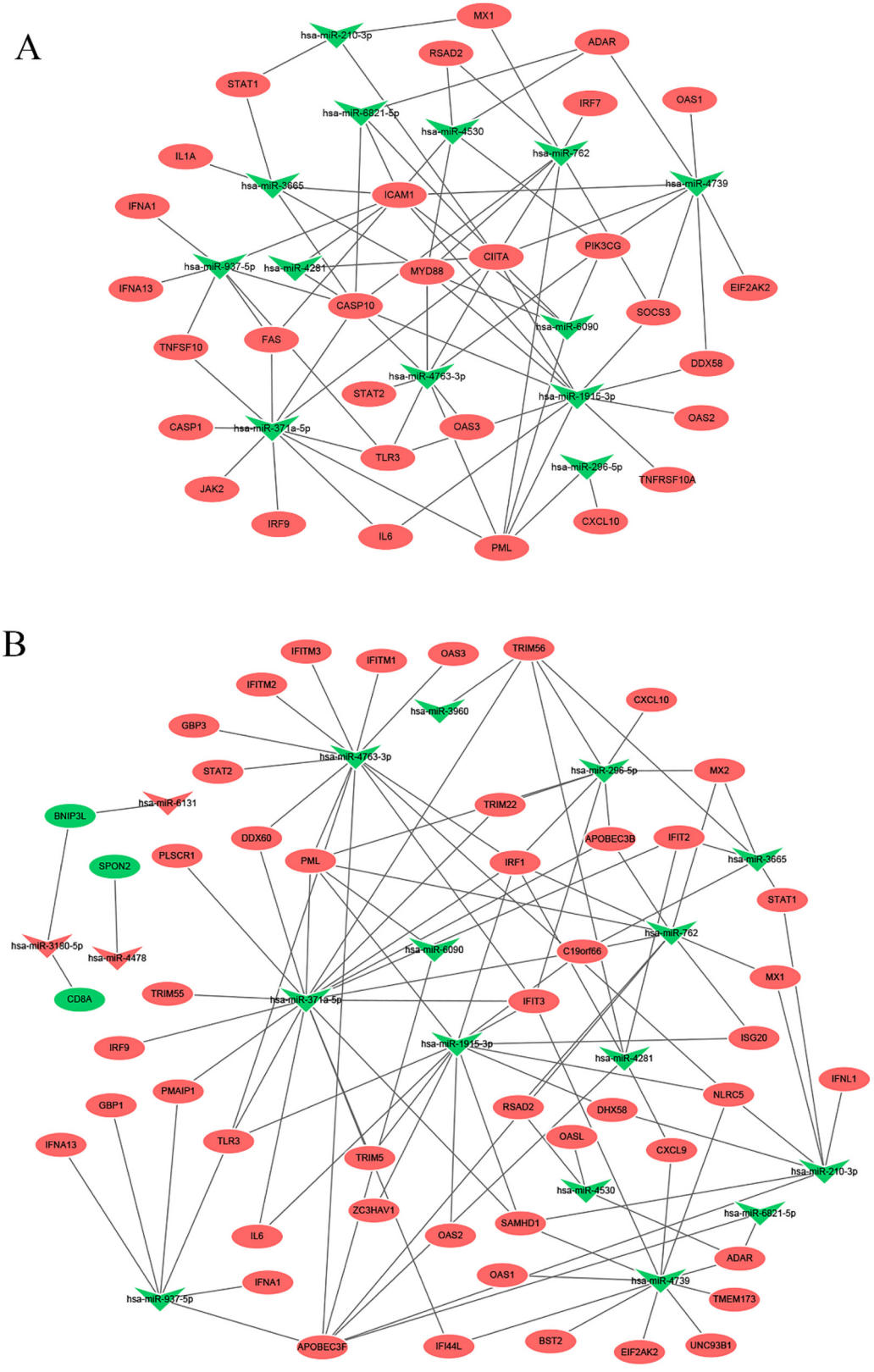

Fig. 6. miRNA-mRNA interaction network and regulatory network in Down syndrome. **A**. Relationships between miRNAs and inversely correlated mRNAs involved in the influenza A pathway. **B**. Relationships between miRNAs and inversely correlated mRNAs involved in the host defense to virus. Green and red represent downregulated and upregulated genes, while triangles and circles represent miRNAs and target gene mRNAs, respectively.

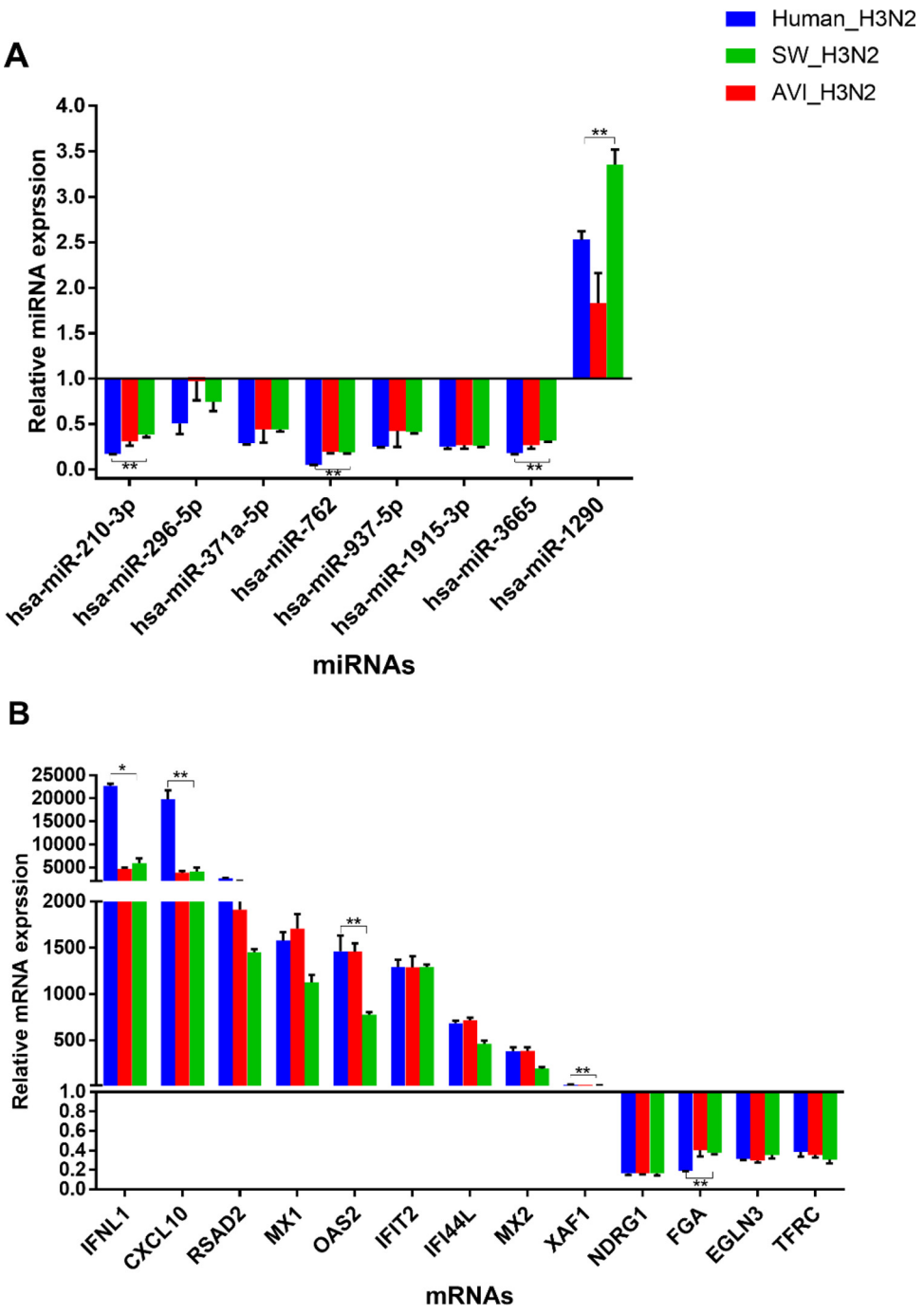

Fig. 7. Validation by RT-qPCR for the DEMs and DEGs that were common to the three infected groups (Human_Br07, AVI_9990, and SW_3861). The expression of 8 miRNAs **(A)** and 13 mRNAs **(B)** identified in the three infected groups was analyzed. The level of expression for uninfected samples was set to one. Relative expression values were normalized to internal standards. The data are expressed as the means ± SD. All experiments (n = 3) were performed in triplicate. Significance is based on one-way ANOVA analyses (*, $P < 0.05$; **, $P < 0.01$). Abbreviations: RT-qPCR: real-time quantitative polymerase chain reaction; DEMs, differentially expressed miRNAs; DEGs, differentially expressed genes.

expression of some miRNAs, which may have broad-spectrum regulation of target genes. Nevertheless, our research has identified different miRNAs than those identified in a similar study performed using the same cell line, with these differences likely being caused by differences in virus samples, sample processing methods or detection techniques. In our study, we used cells infected with three different IAV species to study their differentially expressed miRNAs while also identifying differentially expressed mRNAs using high-throughput sequencing to generate miRNA-mRNA pairs through bioinformatic analyses to screen for miRNAs associated with influenza A infection.

Moreover, the differences in the miRNA expression profiles observed among the cells infected with IAVs of three different origins indicates that they have distinct pathogenicity. First, the number of DEMs identified in the human-origin H3N2 (Human_Br07) infected group was the highest among the three infected groups, a result that has also been observed in numerous previous studies, such as the number of differentially expressed miRNAs in the A-OIV H7N7-infected cells was double that observed in the S-OIV H1N1-infected group (Loveday, Svinti et al. 2012), and H5N1 HPAI IAV infections can cause the greatest number of DEMs compared to infections by pH1N1 and H3N2 influenza viruses (Makkoch, Poomipak et al. 2016). The higher number of DEMs in the human-origin IAV-infected cells suggests that they trigger more genetic changes and cellular pathways than IAVs of other origins. Second, the three IAVs of different origins could induce host cells to produce their own specific miRNAs, which may be highly correlated with the molecular mechanisms of IAVs infection. In a recent report where RT-qPCR was used to detect mature miRNAs from throat swabs of healthy or influenza-infected individuals (25 H1N1, 20 H3N2, 20 influenza B and 21 healthy controls), miR-29a-3p, miR-30c-5p, miR-34c-3p and miR-181a-5p were identified as potentially useful

Table 1
Relationships between 8 miRNAs and inversely correlated 13 target genes selected in RT-qPCR.

miRNA	Target gene
Downregulated	upregulated
hsa-miR-210-3p	MX1, IFNL1
hsa-miR-296-5p	CXCL10, XAF1, MX2
hsa-miR-371a-5p	IFI44 L, XAF1, IFIT2
hsa-miR-762	MX1, MX2,RSAD2
hsa-miR-937-5p	XAF1
hsa-miR-1915-3p	OAS2
hsa-miR-3665	IFIT2, MX2
upregulated	Downregulated
hsa-miR-1290	NDRG1, TFRC, EGLN3, FGA

Results were the predictions of three software programs (TargetScan, microRNAorg, PITA).

biomarkers to differentiate influenza A and B virus-infected patients from healthy controls (Peng et al., 2016). Therefore, miRNAs expressed in response to infection by IAVs of different origins have the potential to be molecular markers for influenza detection. Although this is not the focus of our research, we will continue to analyze the data and elucidate the molecular regulatory mechanisms associated with each specific miRNA, the results of which will be described in a future study. Third, although differentially expressed miRNAs and mRNAs were identified that were common to cells infected by the three assayed IAVs of different origins, the expression levels of some these RNAs differed among the three groups. For instance, the relative expression of hsa-miR-210-3p in cells infected with the human-origin IAV (Human_Br07) was the highest among the three infected groups and was higher in the swine-origin IAV (SW_3861) infected group than in the avian-origin IAV (AVI_9990) infected group. This result was observed in previous studies, where miR-146a was observed to be upregulated in A549 cells infected with H1N1 and H3N2 influenza viruses but was higher in cells infected with H3N2 than in those infected with H1N1 (Terrier et al., 2013). A previous study showed that host genetics may be responsible for this differential regulation in miRNA expression (Bueno et al., 2008), indicating that genetic variation can affect cellar miRNA expression during the influenza virus infection.

Through an integrated analysis of microRNA and mRNA expression, we identified 1852 miRNA-mRNA pairs common to the three infected groups. The results showed that one miRNA could target many mRNAs, and conversely, one mRNA could also be regulated by many miRNAs. For instance, hsa-miR-1290 could upregulate the expression of NDRG1, TFRC, EGLN3, and FGA, while MX2 could be downregulated by hsa-miR-296-5p, hsa-miR-762, and hsa-miR-3665, indicating that these regulatory processes are part of a complex network. Subsequently, a GO analysis was performed to investigate the molecular regulatory mechanisms associated with the miRNA-mRNA pairs. The GO analysis of DEGs shows that human cells primarily use two mechanisms to protect the body from IAV infection: inhibiting viral proliferation and enhancing the immune response by alteration of mRNA expression. The former includes negative regulation of viral genome replication and positive regulation of cellular environmental homeostasis, while the later involves antigen processing and presentation, MHC class I protein complex production, T cell activation, interferon and cytokine production, chemokine activity and the inflammatory response. In our study, approximately 107 identified miRNA-mRNA pairs participate in the defense response to virus, and each of these miRNAs may play a key role in the regulation of specific proteins to inhibit viral infection. Some of these miRNAs may be involved in the inhibition of viral replication. For example, the target prediction analysis indicated that hsa-miR-210-3p may target the IFNL1 gene, and the sequencing and RT-qPCR results demonstrated that hsa-miR-210-3p is differentially downregulated and that IFNL1 is dramatically upregulated in three infection groups (the differential expression of IFNL1 reached 22,746-fold). Interferon lambda-1 (IFNL1) belongs to the Type-III interferon family and is one of the first barriers to influenza virus invasion, interfering with viral replication and gene expression (Killip et al., 2015). Therefore, we hypothesize that miR-210-3p may regulate the expression of IFNL1 to suppress the replication of influenza viruses. However, previous studies observed that the levels of miR-210-3p were significantly higher in patients with congenital cytomegalovirus CMV infection than the control (Kawano et al., 2016), and hsa-miR-210 was upregulated during hepatitis B virus infection (Zhang et al., 2010). Therefore, whether the downregulation of this miRNA during influenza virus infection is unique is worth exploring. In addition, miR-1915-3p may participate as a molecular regulator of Epstein-Barr virus (EBV)-associated gastric cancer (EBVaGC) (Jing et al., 2018). The results of our study show that hsa-miR-1915-3p is differentially downregulated and that its target gene (RSA2) is upregulated, and numerous studies have shown that RSA2 can activate RNase L, leading to the degradation of cellular and viral RNA and inhibiting protein synthesis. Thus, miR-1915-3p may also target the RSA2 gene to terminate viral replication. In contrast, a number of miRNAs can enhance the host immune system to defend against viruses. The target gene prediction analysis showed that CXCL10 may be a target gene of hsa-miR-296-5p. When A549 cells were infected by on the three assayed influenza viruses, the level of CXCL10 was notability higher than that of the negative control, while hsa-miR-296-5p expression was differentially downregulated during this process. The C-X-C motif chemokine ligand 10 (CXCL10) encodes a chemokine of the CXC subfamily and acts as a ligand for the receptor CXCR3 to take part in the defense response to viruses. Some studies have shown that hsa-miR-296-5p suppresses enterovirus 71 replication by targeting the viral genome (Zheng et al., 2013). The results of our study suggest that hsa-miR-296-5p may be involved in controlling IAV infections by indirectly upregulating the expression of CXCL10. Nevertheless, hsa-miR-3180-5p is upregulated and its target gene BNIP3L was downregulated in the three infection groups. BNIP3L encodes a protein that belongs to the pro-apoptotic subfamily within the Bcl-2 family of proteins to induce apoptosis. Although there is no evidence that hsa-miR-3180-5p is associated with IAV infection, the results of our study indicate that hsa-miR-3180-5p may prevent the spread of the virus by inhibiting BNIP3L expression.

In addition, miRNA-mRNA interaction pairs can affect IAV infection by affecting molecular signaling pathways. For example, the KEGG enrichment analysis showed that hsa-miR-296-5p and hsa-miR-3180-5p may target CXCL10 to participate cytokine-cytokine receptor interactions and that hsa-miR-296-5p, hsa-miR-762, and hsa-miR-3665 may target MX2 to participate in the type I interferon signaling pathway, which is essential in the defense against IAV infections. According to the KEGG analysis of DEMs, approximately 39 mRNAs were involved in the influenza A reference pathway, which primarily involves three pathways used to defend against IAV. Notably, hsa-miR-371a-5p, hsa-miR-937-5p, hsa-miR-1915-3p may upregulate the expression of TLR3 to participate in the RIG-I-like receptor signaling pathway, which can stimulate an antiviral response and produce large amounts of interferon to inhibit viral infection. A previous study assessed whether 3p-mNP1496-siRNA targets the influenza NP gene and induces RIG-I activation, the results of which showed that this miRNA can increase the innate immunity of mice infected with IAV (Lin et al., 2012). Previous studies have shown that the use of RIG-I agonists as vaccine adjuvants can enhance the production of anti-influenza virus hemagglutinin (HA)-specific IgG (Martinez-Gil et al., 2013), indicating that these miRNAs involved in the RIG-I-like receptor signaling pathway may be valuable in the exploration of new antiviral targets. In addition, hsa-miR-762, hsa-miR-1915-3p, and hsa-miR-3665 may participate in the Toll-like receptor signaling pathway through upregulation of MYD88 expression. When activated, this pathway has an antiviral role by triggering immune and inflammatory responses. In addition, hsa-miR-1915-3p and hsa-miR-762 may target SOCS3, hsa-miR-371a-5p may target JAK2 and IRF9, and hsa-miR-210-3p may target STAT1 and IFNL1 to take part in

the regulation of the Jak-STAT signaling pathway, which can be suppressed by SOCS-1 to protect cells against viral infection by the overexpression of IFN-λ (Wei et al., 2014). Notably, hsa-miR-296-5p was observed to participate in all the pathways mentioned above by upregulating the expression of CXCL10. Therefore, hsa-miR-296-5p is an important potential antiviral target to combat influenza A infection.

In summary, using microarray and high-throughput sequencing, we performed global miRNA and mRNAs expression profiling in A549 cells infected by IAVs originating from three different species (human H3N2, avian H3N2 and swine H1N1). We identified differentially expressed miRNAs and mRNAs that were common to the three infected groups compared to the uninfected group. We observed that hsa-miR-210-3p, hsa-miR-296-5p, hsa-miR-371a-5p, hsa-miR-762 hsa-miR-937-5p, hsa-miR-1915-3p, hsa-miR-3665 and hsa-miR-1290 were important regulators that may participate in the human defense of IAV infection by regulating the expression of their corresponding mRNAs. Although the mechanisms for the molecular regulation of miRNAs involved in IAV infection remains to be determined, the results of this study provide a foundation for further research of the roles of miRNAs in IAV infection.

Authors' contributions

JG, LXG, RL, ZPL and ZFZ carried out the experiments, JG and LXG analyzed and synthesized the data and wrote the manuscript. XHF designed the study and revised the manuscript. All authors read and approved the final manuscript.

Conflicts of interest

The author(s) declare no potential conflicts of interest with respect to the research, authorship, and/or publication of this article.

Acknowledgements

This study has been supported by National Natural Science Foundation of China (No. 31660040), Innovating Project of Guangxi Graduate Education and YCBZ2014027 from Guangxi Education Department, Young Scientist Foundation of Guangxi Medical University (Grant No. GXMUYSF201525), and Promotion Ability Project of Young Teachers in Guangxi Universities (Grant No. 2018KY0138). The funders had no role in the study design, data collection and analysis, or preparation of the manuscript.

Appendix A. Supplementary data

Supplementary material related to this article can be found, in the online version, at doi:https://doi.org/10.1016/j.virusres.2018.12.016.

References

Anders, S., Pyl, P.T., Huber, W., 2015. HTSeq–a Python framework to work with high-throughput sequencing data. Bioinformatics 31 (2), 166–169. https://doi.org/10.1093/bioinformatics/btu638.

Anders, Simon, Huber, W., 2012. Differential Expression of RNA-Seq Data at the Gene Level –The DESeq Package. European Molecular Biology Laboratory (EMBL).

Bartel, D.P., 2004. MicroRNAs: genomics, biogenesis, mechanism, and function. Cell 116 (2), 281–297.

Bueno, M.J., Perez de Castro, I., Gomez de Cedron, M., Santos, J., Calin, G.A., Cigudosa, J.C., Croce, C.M., Fernandez-Piqueras, J., Malumbres, M., 2008. Genetic and epigenetic silencing of microRNA-203 enhances ABL1 and BCR-ABL1 oncogene expression. Cancer Cell 13 (6), 496–506. https://doi.org/10.1016/j.ccr.2008.04.018.

Buggele, W.A., Johnson, K.E., Horvath, C.M., 2012. Influenza A virus infection of human respiratory cells induces primary microRNA expression. J. Biol. Chem. 287 (37), 31027–31040. https://doi.org/10.1074/jbc.M112.387670.

Carthew, R.W., Sontheimer, E.J., 2009. Origins and mechanisms of miRNAs and siRNAs. Cell 136 (4), 642–655. https://doi.org/10.1016/j.cell.2009.01.035.

Chen, X., Zhou, L., Peng, N., Yu, H., Li, M., Cao, Z., Lin, Y., Wang, X., Li, Q., Wang, J., She, Y., Zhu, C., Lu, M., Zhu, Y., Liu, S., 2017. MicroRNA-302a suppresses influenza A virus-stimulated interferon regulatory factor-5 expression and cytokine storm induction. J. Biol. Chem. 292 (52), 21291–21303. https://doi.org/10.1074/jbc.M117.805937.

Deng, Y., Yan, Y., Tan, K.S., Liu, J., Chow, V.T., Tao, Z.Z., Wang, D.Y., 2017. MicroRNA-146a induction during influenza H3N2 virus infection targets and regulates TRAF6 levels in human nasal epithelial cells (hNECs). Exp. Cell Res. 352 (2), 184–192. https://doi.org/10.1016/j.yexcr.2017.01.011.

Grundhoff, A., Sullivan, C.S., 2011. Virus-encoded microRNAs. Virology 411 (2), 325–343. https://doi.org/10.1016/j.virol.2011.01.002.

Hill, M., Tran, N., 2018. MicroRNAs regulating microRNAs in cancer. Trends Cancer 4 (7), 465–468. https://doi.org/10.1016/j.trecan.2018.05.002.

Holla, S., Balaji, K.N., 2015. Epigenetics and miRNA during bacteria-induced host immune responses. Epigenomics 7 (7), 1197–1212. https://doi.org/10.2217/epi.15.75.

Jing, J.J., Wang, Z.Y., Li, H., Sun, L.P., Yuan, Y., 2018. Key elements involved in Epstein-Barr virus-associated gastric cancer and their network regulation. Cancer Cell Int. 18, 146. https://doi.org/10.1186/s12935-018-0637-5.

Kanehisa, M., Araki, M., Goto, S., Hattori, M., Hirakawa, M., Itoh, M., Katayama, T., Kawashima, S., Okuda, S., Tokimatsu, T., Yamanishi, Y., 2008. KEGG for linking genomes to life and the environment. Nucleic Acids Res. 36 (Database issue), D480–484. https://doi.org/10.1093/nar/gkm882.

Kawano, Y., Kawada, J., Kamiya, Y., Suzuki, M., Torii, Y., Kimura, H., Ito, Y., 2016. Analysis of circulating human and viral microRNAs in patients with congenital cytomegalovirus infection. J. Perinatol. 36 (12), 1101–1105. https://doi.org/10.1038/jp.2016.157.

Khongnomnan, K., Makkoch, J., Poomipak, W., Poovorawan, Y., Payungporn, S., 2015. Human miR-3145 inhibits influenza A viruses replication by targeting and silencing viral PB1 gene. Exp. Biol. Med. 240 (12), 1630–1639. https://doi.org/10.1177/1535370215589051.

Killip, M.J., Fodor, E., Randall, R.E., 2015. Influenza virus activation of the interferon system. Virus Res. 209, 11–22. https://doi.org/10.1016/j.virusres.2015.02.003.

Kim, D., Langmead, B., Salzberg, S.L., 2015. HISAT: a fast spliced aligner with low memory requirements. Nat. Methods.

Kuiken, T., Holmes, E.C., McCauley, J., Rimmelzwaan, G.F., Williams, C.S., Grenfell, B.T., 2006. Host species barriers to influenza virus infections. Science 312 (5772), 394–397. https://doi.org/10.1126/science.1122818.

Li, X., Fu, Z., Liang, H., Wang, Y., Qi, X., Ding, M., Sun, X., Zhou, Z., Huang, Y., Gu, H., Li, L., Chen, X., Li, D., Zhao, Q., Liu, F., Wang, H., Wang, J., Zen, K., Zhang, C.Y., 2018. H5N1 influenza virus-specific miRNA-like small RNA increases cytokine production and mouse mortality via targeting poly(rC)-binding protein 2. Cell Res. 28 (2), 157–171. https://doi.org/10.1038/cr.2018.3.

Lin, L., Liu, Q., Berube, N., Detmer, S., Zhou, Y., 2012. 5'-Triphosphate-short interfering RNA: potent inhibition of influenza A virus infection by gene silencing and RIG-I activation. J. Virol. 86 (19), 10359–10369. https://doi.org/10.1128/JVI.00665-12.

Lin, J., Xia, J., Chen, Y.T., Zhang, K.Y., Zeng, Y., Yang, Q., 2017. H9N2 avian influenza virus enhances the immune responses of BMDCs by down-regulating miR29c. Vaccine 35 (5), 729–737. https://doi.org/10.1016/j.vaccine.2016.12.054.

Livak, K.J., Schmittgen, T.D., 2001. Analysis of relative gene expression data using real-time quantitative PCR and the 2(-Delta Delta C(T)) Method. Methods 25 (4), 402–408. https://doi.org/10.1006/meth.2001.1262.

Loveday, E.K., Svinti, V., Diederich, S., Pasick, J., Jean, F., 2012. Temporal- and strain-specific host microRNA molecular signatures associated with swine-origin H1N1 and avian-origin H7N7 influenza A virus infection. J. Virol. 86 (11), 6109–6122. https://doi.org/10.1128/JVI.06892-11.

Ma, Y.J., Yang, J., Fan, X.L., Zhao, H.B., Hu, W., Li, Z.P., Yu, G.C., Ding, X.R., Wang, J.Z., Bo, X.C., Zheng, X.F., Zhou, Z., Wang, S.Q., 2012. Cellular microRNA let-7c inhibits M1 protein expression of the H1N1 influenza A virus in infected human lung epithelial cells. J. Cell. Mol. Med. 16 (10), 2539–2546. https://doi.org/10.1111/j.1582-4934.2012.01572.x.

Maemura, T., Fukuyama, S., Sugita, Y., Lopes, T.J.S., Nakao, T., Noda, T., Kawaoka, Y., 2018. Lung-derived exosomal miR-483-3p regulates the innate immune response to influenza virus infection. J. Infect. Dis. 217 (9), 1372–1382. https://doi.org/10.1093/infdis/jiy035.

Makkoch, J., Poomipak, W., Saengchoowong, S., Khongnomnan, K., Praianantathavorn, K., Jinato, T., Poovorawan, Y., Payungporn, S., 2016. Human microRNAs profiling in response to influenza A viruses (subtypes pH1N1, H3N2, and H5N1). Exp. Biol. Med. 241 (4), 409–420.

Martinez-Gil, L., Goff, P.H., Hai, R., Garcia-Sastre, A., Shaw, M.L., Palese, P., 2013. A Sendai virus-derived RNA agonist of RIG-I as a virus vaccine adjuvant. J. Virol. 87 (3), 1290–1300. https://doi.org/10.1128/JVI.02338-12.

Nicholson, K.G., Wood, J.M., Zambon, M., 2003. Influenza. Lancet 362 (9397), 1733–1745. https://doi.org/10.1016/S0140-6736(03)14854-4.

Patel, R.K., Jain, M., 2012. NGS QC Toolkit: a toolkit for quality control of next generation sequencing data. PLoS One 7 (2), e30619. https://doi.org/10.1371/journal.pone.0030619.

Peng, F., He, Ja., Loo, J.F.C., Kong, S.K., Li, B., Gu, D., 2017. Identification of serum MicroRNAs as diagnostic biomarkers for influenza H7N9 infection. Virol. Rep. 7, 1–8. https://doi.org/10.1016/j.virep.2016.11.001.

Peng, S., Wang, J., Wei, S., Li, C., Zhou, K., Hu, J., Ye, X., Yan, J., Liu, W., Gao, G.F., Fang, M., Meng, S., 2018. Endogenous Cellular microRNAs mediate antiviral defense against influenza A virus. Molecular therapy. Nucleic Acids 10, 361–375. https://doi.org/10.1016/j.omtn.2017.12.016.

Roberts, A., Trapnell, C., Donaghey, J., Rinn, J.L., Pachter, L., 2011. Improving RNA-Seq expression estimates by correcting for fragment bias. Genome Biol. 12 (3), R22. https://doi.org/10.1186/gb-2011-12-3-r22.

Rosenberger, C.M., Podyminogin, R.L., Diercks, A.H., Treuting, P.M., Peschon, J.J., Rodriguez, D., Gundapuneni, M., Weiss, M.J., Aderem, A., 2017. miR-144 attenuates the host response to influenza virus by targeting the TRAF6-IRF7 signaling axis. PLoS Pathog. 13 (4), e1006305. https://doi.org/10.1371/journal.ppat.1006305.

Shih, S.-r.T., Chen, C.-j.T., Huang, S.-y.T., 2017. Method of treating influenza A Source Google Patents. United States Patent.

Short, K.R., Richard, M., Verhagen, J.H., van Riel, D., Schrauwen, E.J., van den Brand, J.M., Manz, B., Bodewes, R., Herfst, S., 2015. One health, multiple challenges: The inter-species transmission of influenza A virus. One Health 1, 1–13. https://doi.org/10.1016/j.onehlt.2015.03.001.

Song, L., Liu, H., Gao, S., Jiang, W., Huang, W., 2010. Cellular microRNAs inhibit replication of the H1N1 influenza A virus in infected cells. J. Virol. 84 (17), 8849–8860. https://doi.org/10.1128/JVI.00456-10.

Sun, X., Pulit-Penaloza, J.A., Belser, J.A., Pappas, C., Pearce, M.B., Brock, N., Zeng, H., Creager, H.M., Zanders, N., Jang, Y., Tumpey, T.M., Davis, T., Maines, T.R., 2018. Pathogenesis and transmission of genetically diverse swine-origin H3N2v influenza A viruses from multiple lineages isolated in the United States, 2011-2016. J. Virol. https://doi.org/10.1128/JVI.00665-18.

Terrier, O., Textoris, J., Carron, C., Marcel, V., Bourdon, J.C., Rosa-Calatrava, M., 2013. Host microRNA molecular signatures associated with human H1N1 and H3N2 influenza A viruses reveal an unanticipated antiviral activity for miR-146a. J. Gen. Virol. 94 (Pt 5), 985–995. https://doi.org/10.1099/vir.0.049528-0.

Trapnell, C., Williams, B.A., Pertea, G., Mortazavi, A., Kwan, G., van Baren, M.J., Salzberg, S.L., Wold, B.J., Pachter, L., 2010. Transcript assembly and quantification by RNA-Seq reveals unannotated transcripts and isoform switching during cell differentiation. Nat. Biotechnol. 28 (5), 511–515. https://doi.org/10.1038/nbt.1621.

Trobaugh, D.W., Klimstra, W.B., 2017. MicroRNA regulation of RNA virus replication and pathogenesis. Trends Mol. Med. 23 (1), 80–93. https://doi.org/10.1016/j.molmed.2016.11.003.

Turchinovich, A., Weiz, L., Burwinkel, B., 2012. Extracellular miRNAs: the mystery of their origin and function. Trends Biochem. Sci. 37 (11), 460–465. https://doi.org/10.1016/j.tibs.2012.08.003.

Van Reeth, K., 2007. Avian and swine influenza viruses: our current understanding of the zoonotic risk. Vet. Res. 38 (2), 243–260. https://doi.org/10.1051/vetres:2006062.

Wang, R., Zhang, Y.Y., Lu, J.S., Xia, B.H., Yang, Z.X., Zhu, X.D., Zhou, X.W., Huang, P.T., 2017. The highly pathogenic H5N1 influenza A virus down-regulated several cellular MicroRNAs which target viral genome. J. Cell. Mol. Med. 21 (11), 3076–3086. https://doi.org/10.1111/jcmm.13219.

Wei, H., Wang, S., Chen, Q., Chen, Y., Chi, X., Zhang, L., Huang, S., Gao, G.F., Chen, J.L., 2014. Suppression of interferon lambda signaling by SOCS-1 results in their excessive production during influenza virus infection. PLoS Pathog. 10 (1), e1003845. https://doi.org/10.1371/journal.ppat.1003845.

Xia, B., Lu, J., Wang, R., Yang, Z., Zhou, X., Huang, P., 2018. miR-21-3p Regulates influenza A virus replication by targeting histone deacetylase-8. Front. Cell. Infect. Microbiol. 8, 175. https://doi.org/10.3389/fcimb.2018.00175.

Zhang, G.L., Li, Y.X., Zheng, S.Q., Liu, M., Li, X., Tang, H., 2010. Suppression of hepatitis B virus replication by microRNA-199a-3p and microRNA-210. Antiviral Res. 88 (2), 169–175. https://doi.org/10.1016/j.antiviral.2010.08.008.

Zhang, S., Wang, R., Su, H., Wang, B., Sizhu, S., Lei, Z., Jin, M., Chen, H., Cao, J., Zhou, H., 2017. Sus scrofa miR-204 and miR-4331 negatively regulate swine H1N1/2009 influenza A virus replication by targeting viral HA and NS, respectively. Int. J. Mol. Sci. 18 (4), E749. https://doi.org/10.3390/ijms18040749.

Zhang, S., Li, J., Li, J., Yang, Y., Kang, X., Li, Y., Wu, X., Zhu, Q., Zhou, Y., Hu, Y., 2018a. Up-regulation of microRNA-203 in influenza A virus infection inhibits viral replication by targeting DR1. Sci. Rep. 8 (1), 6797. https://doi.org/10.1038/s41598-018-25073-9.

Zhang, Y., Yun, Z., Gong, L., Qu, H., Duan, X., Jiang, Y., Zhu, H., 2018b. Comparison of miRNA evolution and function in plants and animals. MicroRNA 7 (1), 4–10. https://doi.org/10.2174/2211536607666180126163031.

Zheng, Z., Ke, X., Wang, M., He, S., Li, Q., Zheng, C., Zhang, Z., Liu, Y., Wang, H., 2013. Human microRNA hsa-miR-296-5p suppresses enterovirus 71 replication by targeting the viral genome. J. Virol. 87 (10), 5645–5656. https://doi.org/10.1128/JVI.02655-12.

Zhou, L., Chen, E., Bao, C., Xiang, N., Wu, J., Wu, S., Shi, J., Wang, X., Zheng, Y., Zhang, Y., Ren, R., Greene, C.M., Havers, F., Iuliano, A.D., Song, Y., Li, C., Chen, T., Wang, Y., Li, D., Ni, D., Zhang, Y., Feng, Z., Uyeki, T.M., Li, Q., 2018. Clusters of human infection and human-to-human transmission of avian influenza A(H7N9) virus, 2013-2017. Emerg. Infect. Dis. 24 (2). https://doi.org/10.3201/eid2402.171565.